Optical coordinate transformations

N. Davidson, A. A. Friesem, and E. Hasman

A novel technique for designing holographic optical elements that can perform general types of coordinate transformation is presented. The design is based on analytic ray-tracing techniques for finding the grating vector of the element, from which the holographic grating function is obtained as a solution of a Poissonlike equation. The grating function can be formed either as a computer-generated or as a computer-originated hologram. The design and realization procedure are illustrated for a specific holographic element that performs a logarithmic coordinate transformation on two-dimensional patterns.

Introduction

The design and use of holographic optical elements (HOE's) to perform coordinate transformations were first suggested by Bryngdahl.[1] Transformations with HOE's were exploited for distortion compensation,[2] for angle multiplexing in optical fibers,[3] and for optical data processing.[4,5] The design of HOE's for these transformations is based on two approximations: the saddle-point approximation and the paraxial approximation. These approximations impose contradicting requirements on the distance between the input and the output planes. The saddle-point approximation calls for a short distance compared to the lateral dimensions, whereas the paraxial approximation requires the distance to be much longer. Such contradicting requirements impose severe limitations on the space–bandwidth product (SBP) of the data that may be transformed without degradations.[6] Furthermore, these design procedures were suitable only for certain types of transformation.[6] For more general transformations, faceted HOE's with even lower SBP capabilities[7] or complex optical systems containing two HOE's in cascade[8] have been suggested.

In this paper we present a new procedure for designing HOE's without the need for paraxial approximation. In this procedure, analytic ray-tracing techniques are first exploited to determine the necessary grating vector, from which the optimal grating function for forming the HOE's is derived by variational methods. With such grating functions, the SBP of the data that can be transformed is significantly improved, and the coordinate transformation need not be limited to a specific type. Furthermore, the Fourier transform lenses that were included in the earlier designs need no longer be added.

In the following we show how to obtain both the grating vector and the grating function of the HOE and how to evaluate the SBP capabilities of the coordinate transformations. Finally, the procedure is illustrated by designing and testing a HOE for two-dimensional logarithmic transformation. Such a transformation is useful for scale-invariant optical correlators.[6]

Design of the Holographic Grating Vector

An optical arrangement for realizing a general two-dimensional coordinate transformation $(x, y) \rightarrow [u(x, y), v(x, y)]$ is shown in Fig. 1. The input object, a transparency or a spatial light modulator with an amplitude transmission function of $t(x, y)$, is placed adjacent to a HOE having a grating function of $\phi_h(x, y)$, and illuminated by a coherent plane wave. The desired coordinate transformation $T(u, v)$ is obtained at some distance z away. To find the necessary grating function for the HOE, it is most convenient to find its grating vector first.[9] This is best done by exploiting the propagation vectors of the input and output wave fronts.[9]

The normalized propagation vectors, which can be regarded as the direction cosines of the input ($\mathbf{K}_i$) and output ($\mathbf{K}_o$) rays, can be written as

$$\mathbf{K}_i = \frac{\lambda}{2\pi}\nabla\phi_i, \quad \mathbf{K}_o = \frac{\lambda}{2\pi}\nabla\phi_o, \tag{1}$$

and the grating vector $\mathbf{K}_h$, as

$$\mathbf{K}_h = \frac{\lambda}{2\pi}\nabla\phi_h = K_{h_x}\hat{x} + K_{h_y}\hat{y} = \frac{\lambda}{\Lambda_x}\hat{x} + \frac{\lambda}{\Lambda_y}\hat{y}, \tag{2}$$

The authors are with the Department of Electronics, Weizmann Institute of Science, Rehovot 76100, Israel.

Received 4 January 1991.
0003-6935/92/081067-07$05.00/0.

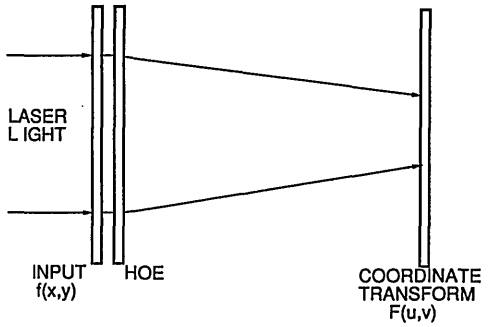

Fig. 1. Coordinate transformation arrangement with a HOE.

where ∇ is the gradient operator, ϕ_i and ϕ_o are the phases of the input and output wave fronts, respectively, λ is the wavelength of light, and Λ_x and Λ_y are the grating periods in the x and y directions. The diffraction relation for the first diffraction order of the HOE can now be written as

$$\begin{aligned} K_{o_x} &= K_{i_x} + K_{h_x}, \\ K_{o_y} &= K_{i_y} + K_{h_y}, \\ K_{o_z} &= (1 - K_{o_x}^2 - K_{o_y}^2)^{1/2} \end{aligned} \tag{3}$$

The HOE can thus be viewed as a combination of local gratings that change the direction of the incident rays of light according to Eqs. (3).

We proceed by assuming that diffraction by the input pattern can be neglected; this assumption can be shown to hold true when the distance between the input and the output planes is small compared to $\lambda^{-1} f_{\max}^2$, where $f_{\max}$ is the maximal spatial frequency of the input.[10] Thus, a ray of light traversing from the point $(x, y, z = 0)$ on the HOE to the output plane at the coordinates (u, v, z) should have the propagation vectors

$$\begin{aligned} K_{o_x}(x, y) &= \frac{u(x, y) - x}{r}, \\ K_{o_y}(x, y) &= \frac{v(x, y) - y}{r}, \end{aligned} \tag{4}$$

where

$$r^2 = [u(x, y) - x]^2 + [v(x, y) - y]^2 + z^2.$$

Assuming an incident input plane wave at an off-axis angle α_i in the x–z plane [i.e., $\mathbf{K}_{i_x} = \sin(\alpha_i)$ and $\mathbf{K}_{i_y} = 0$] and inserting Eqs. (4) into Eqs. (3) yield the desired grating vectors:

$$\begin{aligned} K_{h_x}(x, y) &= \frac{u(x, y) - x}{r} - \sin(\alpha_i), \\ K_{h_y}(x, y) &= \frac{v(x, y) - y}{r}. \end{aligned} \tag{5}$$

Equations (5) can also be derived in terms of wave optics. The light amplitude in the output plane of the optical arrangement shown in Fig. 1 can be written by exploiting the Fresnel–Kirchhoff integral[10]:

$$T(u, v, z) = \int_{-\infty}^{+\infty} \int_{-\infty}^{+\infty} dx dy \{g(x, y) \exp[ikh(x, y)]\},$$

where

$$\begin{aligned} g(x, y) &= \frac{z}{i\lambda r^2} t(x, y), \\ h(x, y) &= \hat{\phi}_h(x, y) + r, \end{aligned} \tag{6}$$

and $\hat{\phi}_h = (\lambda/2\pi)\phi_h$ is the normalized grating function, $k = 2\pi/\lambda$ is the wave number, z/r^2 is the inclination factor,[10] and an on-axis incoming wave ($\alpha_i = 0$) was assumed. For typical optical wavelengths k is large and the integral can be fairly well approximated by using the standard saddle-point method,[11] which specifies that the main contribution to the integral is provided from the saddle points of the phase function $h(x, y)$, for which

$$\frac{\partial h}{\partial x} = \frac{\partial h}{\partial y} = 0. \tag{7}$$

Applying these relations to Eqs. (6) yields the following conditions on the holographic grating vector:

$$\begin{aligned} K_{h_x}(x, y) &= \frac{\partial \hat{\phi}_h}{\partial x} = -\frac{\partial r}{\partial x} = \frac{u(x, y) - x}{r}, \\ K_{h_y}(x, y) &= \frac{\partial \hat{\phi}_h}{\partial y} = -\frac{\partial r}{\partial y} = \frac{v(x, y) - y}{r}. \end{aligned} \tag{8}$$

This condition ensures that the main energy contribution to the point (u, v) in the output plane comes from the point (x, y) in the input plane, having the grating vector $\mathbf{K}_h$ of Eqs. (5) as derived by means of geometrical optics.

The light amplitude in the output plane within the saddle-point approximation is given by[11]

$$\begin{aligned} T(u, v, z) \approx t(x_s, y_s) &\exp\left\{i\left[kh(x_s, y_s) + \frac{\pi}{4}\right]\right\} \\ &\times (h_{xx} h_{yy} - h_{xy}^2)^{-1/2} \frac{z}{r(x_s, y_s)^2}, \end{aligned} \tag{9}$$

where (x_s, y_s) is the saddle point for which Eq. (7) is fulfilled, and the notation $h_{xx} = \partial^2 h/\partial x^2$, etc. is used. This expression is indeed the desired coordinate transformation $t(x, y) \rightarrow T[u(x, y), v(x, y)]$ provided that Eqs. (8) are fulfilled, but the transformed function is multiplied by a phase function and an amplitude function. The phase function $\exp\{i[kh(x_s, y_s) + (\pi/4)]\}$ can be corrected, if needed, by a second HOE. However, in many cases the output plane is detected by a square-law detector, and the phase term is not important. The amplitude term, $(h_{xx} h_{yy} - h_{xy}^2)^{-1/2} z/r^2$, can be discarded by an appropriate amplitude mask either in the input or in the output planes (it is possible also to incorporate the amplitude mask and the phase mask into a single HOE). Note that, for the paraxial case, this amplitude term converges to the

Jacobian of the transformation and expresses the fact that energy is conserved by the transformation.

Holographic Grating Function

The grating function $\phi(x, y)$ can be found, in general, by exploiting the relation

$$\nabla\phi_h(x, y) = \frac{2\pi}{\lambda}\mathbf{K}_h(x, y). \tag{10}$$

For one-dimensional elements, the grating function is given by

$$\phi_h(x) = \frac{2\pi}{\lambda}\int \mathbf{K}_h(x')dx', \tag{11}$$

where the constant of integration can be chosen arbitrarily. For two-dimensional elements (the 2-D case), a unique solution is possible if the following condition is fulfilled:

$$\frac{\partial K_{h_x}(x, y)}{\partial y} = \frac{\partial K_{h_y}(x, y)}{\partial x}. \tag{12}$$

A vector that fulfills this condition is known as a conserving vector.

Let us examine some special cases where the condition of Eq. (12) is fulfilled. When the desired coordinate transformation has circular symmetry, i.e., ρ is transformed to $w(\rho)$, where $\rho = (x^2 + y^2)^{1/2}$, the 2-D situation is essentially comparable to the one-dimensional case after exchanging x with ρ, so the grating function can be found as in Eq. (11). Alternatively, when the coordinate transformation is separable, i.e., (x, y) is transformed to $[u(x), v(y)]$, the paraxial approximation can be exploited to replace r by z in Eq. (5), yielding a grating vector of the form $K_{h_x}(x)\hat{x} + K_{h_y}(y)\hat{y}$, thereby fulfilling the condition of Eq. (12). The grating function is thus

$$\phi_h(x, y) = \frac{2\pi}{\lambda}\int K_{h_x}(x')dx' + \frac{2\pi}{\lambda}\int K_{h_y}(y')dy'. \tag{13}$$

When the paraxial approximation is not valid, it is still possible to get an analytic grating function by obtaining the transformation in two stages as shown in Fig. 2. In the first stage (x, y) is transformed to $[u(x), y]$, so the grating vector is only x dependent and Eq. (12) is valid. In the second stage $[u(x), y]$ is transformed to $[u(x), v(y)]$ and the grating vector has the form

$$\mathbf{K}_h = K_{h_x}(x)\hat{x} + K_{h_y}(y)\hat{y}, \tag{14}$$

where $K_{h_x}(x)$ is the negative of the grating vector of the first stage. This grating vector fulfills the condition of Eq. (12), and the grating function can be obtained by Eq. (13). This decomposition approach may also be applied to some nonseparable coordinate transformations.[8]

In the general case when the grating vector is not a conserving vector, there is no analytical grating function that fulfills Eq. (10). For this case we try to determine the best grating function ϕ_h, in the sense that its gradient is closest to the desired grating vector $(\mathbf{K}_{h_x}, \mathbf{K}_{h_y})$ of Eqs. (5). Specifically, we use l_2 metric in the Hilbert space of 2-D functions and minimize the following functional of $\phi_h(x, y)$:

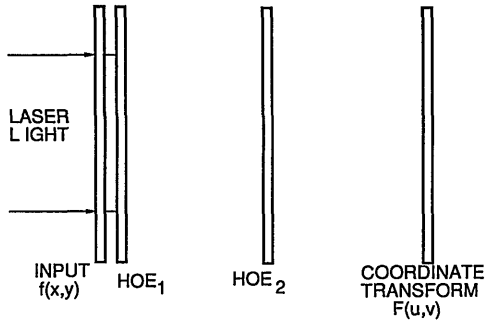

Fig. 2. Optical arrangement for separable 2-D coordinate transformations. The first HOE performs the x-coordinate transformation and the second HOE performs the y-coordinate transformation.

$$L[\phi_h(x, y)] = \int_A\int dxdy\left[\left(\frac{\partial\phi_h}{\partial x} - \frac{2\pi}{\lambda}\mathbf{K}_{h_x}\right)^2 + \left(\frac{\partial\phi_h}{\partial y} - \frac{2\pi}{\lambda}\mathbf{K}_{h_y}\right)^2\right], \tag{15}$$

where the integration is over the area A of the HOE. The minimization is performed by solving the Legendre equation:

$$\frac{\delta L[\phi_h(x, y)]}{\delta\phi_h(x, y)} = 0, \tag{16}$$

where δ indicates a functional derivative.

Now the functional is of the form

$$L = \int\int dxdy\left[F\left(x, y, \phi_h, \frac{\partial\phi_h}{\partial x}, \frac{\partial\phi_h}{\partial y}\right)\right]. \tag{17}$$

Consequently, Eq. (16) can be expressed as a Euler equation[12]:

$$\frac{\delta F}{\delta\phi_h} - \frac{\delta}{\delta x}\frac{\delta F}{\delta(\partial\phi_h/\partial x)} - \frac{\delta}{\delta y}\frac{\delta F}{\delta(\partial\phi_h/\partial y)} = 0. \tag{18}$$

Incorporating the specific functional L from Eq. (15) into Eqs. (17) and (18) yields the Poissonlike relation

$$\nabla^2\phi = \frac{2\pi}{\lambda}\,\mathrm{div}(\mathbf{K}_h), \tag{19}$$

where $\nabla^2 = (\partial^2/\partial x^2) + (\partial^2/\partial y^2)$ and div are the Laplacian and divergence operators, respectively. Substituting the general transformation $(x, y) \rightarrow (u, v)$ for $\mathbf{K}_h$ from Eq. (5) into Eq. (19) yields

$$\nabla^2\phi = \frac{2\pi}{\lambda r^3}\left\{\left(\frac{\partial u}{\partial x} - 1\right)[z^2 + (v - y)^2] + \left(\frac{\partial v}{\partial y} - 1\right)[z^2 + (u - x)^2] - (u - x)(v - y)\left(\frac{\partial u}{\partial y} + \frac{\partial v}{\partial x}\right)\right\}. \tag{20}$$

This equation can be solved numerically by using standard computer programs where (a) the proper boundary conditions are $\partial\phi_h/\partial\mathbf{n} = \mathbf{K}_h$ on the boundary of the HOE with $\mathbf{n}$ as a unit vector normal to the boundary, and (b) the constant of integration can be arbitrarily chosen. Note, for geometries in which the paraxial approximation is valid, Eq. (20) can be simplified to yield

$$\nabla^2\phi = \frac{2\pi}{\lambda z}\left(\frac{\partial u}{\partial x} + \frac{\partial v}{\partial y} - 2\right). \tag{21}$$

Space–Bandwidth Product Considerations

The performance criteria of the HOE for coordinate transformations can be characterized by the maximal SBP of the input that can be transformed without severe distortions (SBP_{ct}). For simplicity we determine the SBP_{ct} for the one-dimensional case (for two dimensions, the SBP of the one-dimensional case should be squared). In our derivation, we consider only diffraction effects. Other effects, such as those caused by the difference between $\nabla\phi_h$ and a nonconserving grating vector, should be addressed separately for any specific transformation.

For the paraxial case (i.e., where the distance z is much larger than the input size), the minimal pixel size possible, p, can be determined by the geometric shadow condition $\lambda z \approx p^2$, where λ is the wavelength and z is the distance between the input and output planes.[10] Using this relation, for coordinate transformations we can write

$$\mathrm{SBP}_{ct} \equiv \frac{D}{p} \approx \sqrt{\frac{D^2}{\lambda z}} = \sqrt{\frac{D}{\lambda F_\#}} = \sqrt{\mathrm{SBP}_{\mathrm{imag}}}, \tag{22}$$

where D is the total width of the input, $F_\# = z/D$, and SBP_{imag} is the diffraction-limited SBP of an aberration-free imaging system having the same $F_\#$. Equation (22) indicates that the SBP of the coordinate transformation system (SBP_{ct}) is comparable to the square root of the SBP for an ideal imaging system (SBP_{imag}). This conclusion is in agreement with the fact that the number of degrees of freedom for space-variant operators is the square of the number of degrees of freedom for space-invariant operators.[13] It is worthwhile noting that Eq. (22) is also valid for the coordinate transformation HOE's that were originally suggested by Bryngdahl,[1] except that there the $F_\#$ refers to a Fourier-transform lens that must be added. Consequently, to avoid severe aberrations, the $F_\#$ must be relatively high.

For the general nonparaxial case (i.e., low $F_\#$), we begin by considering a beam incident on a small pixel aperture of width p, at an inclination angle α, as shown in Fig. 3, where only the center ray of the beam, traversing from point x to point $u(x)$, is shown. The diffraction widening of the beam at the output plane located at a distance z from the aperture is[14]

$$\xi = \frac{\lambda r}{p}\frac{1}{\cos^2\alpha}, \tag{23}$$

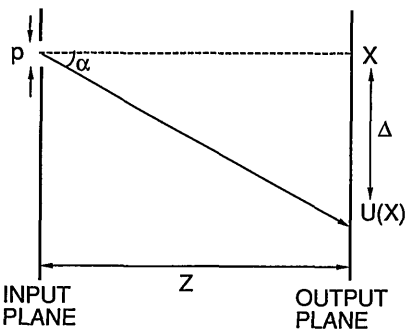

Fig. 3. Geometry of the coordinate transformation with high inclination angles.

where p is the width of the aperture, $r = (\Delta^2 + z^2)^{1/2}$ is the slant distance with the lateral shift $\Delta = u(x) - x$, and the $1/\cos^2\alpha$ term is due to the projection of the input and output planes on the plane vertical to the beam propagating direction with $\alpha = \tan^{-1}(\Delta/z)$ as the inclination angle. [Note that in the paraxial case Eq. (23) simplifies to the well-known $\lambda z/p$ diffraction widening.] For a given Δ, the least diffraction widening is obtained at a distance z_{opt} for which $\partial\xi/\partial z = 0$. This yields

$$z_{opt} = \sqrt{2}\Delta. \tag{24}$$

Equation (24) implies that, for coordinate transformation, SBP_{ct} will be maximized when the distance between the input and the output planes, z, is equal to $1.41\Delta_{max}$, where Δ_{max} is the maximal lateral displacement. Using this conclusion yields

$$\mathrm{SBP}_{ct}(z = z_{opt}) \approx \left(\frac{D^2}{1.41\lambda\Delta_{max}}\right)^{1/2} = \left(\frac{D}{1.41\lambda\eta}\right)^{1/2}, \tag{25}$$

where $\eta = \Delta_{max}/D$ is a dimensionless number that characterizes the amount of distortion of the specific transformation. For the worst case of $\eta = 1$ (transformations with high distortion), SBP_{ct} is only D/λ, which is comparable to using $F_\# = 1$ in Eq. (22). However, in many cases $\eta \ll 1$ (transformations with low distortion), so SBP_{ct} is greatly increased.

In general, the HOE's for coordinate transformations are recorded as computer-generated holograms (CGH's). As a result, the SBP_{ct} is often limited by the resolving capabilities (or SBP) of the plotters that are used to record the CGH's. To determine this limitation we begin by expressing the maximal diffraction angle of the HOE, α_{max}, as

$$\alpha_{max} = \arcsin(\lambda/\Lambda_{min}), \tag{26}$$

where Λ_{min} is the minimal grating spacing limited by the finite resolution of the plotter. From geometric considerations (see Fig. 3),

$$\tan(\alpha_{max}) \approx \frac{s\Delta_{max}}{z} = \frac{s\eta D}{z}, \tag{27}$$

where the constant s is due to the off-axis linear term

that must be added to the grating function when it is necessary to separate the different diffraction orders. When the HOE is recorded as a kinoform (only one order is diffracted), there is no need for separation of orders, so $s = 1$. When the HOE is recorded directly as a binary CGH, the different orders must be separated at the output plane, at a distance z from the HOE, and s should be taken as $s = 1 + (1/\eta)$. Finally, when the HOE is recorded as a computer-originated hologram (COH),[15] where the linear phase is added by interfering the wave front that emerges from a CGH with an off-axis plane wave, the separation of the orders is done in the Fourier plane, so $s = 2$.

Combining Eq. (26) and approximation (27) with $s = 2$ and using the paraxial approximation of $\alpha \approx \sin\alpha \approx \tan\alpha$ yield

$$F_{\#\min} \approx \frac{2\eta\Lambda_{\min}}{\lambda}. \tag{28}$$

Substituting approximation (28) into Eq. (22) gives the final result:

$$\max(\mathrm{SPB}_{ct}) \approx \left(\frac{D}{2\eta\Lambda_{\min}}\right)^{1/2} = \left(\frac{\mathrm{SBP}_{\mathrm{plot}}}{2\eta}\right)^{1/2}, \tag{29}$$

where $\mathrm{SBP}_{\mathrm{plot}} = D/\Lambda_{\min}$ denotes the SBP of the plotter. By comparing approximations (25) and (29), it is clear that, when $2\Lambda_{\min}$ is larger than $\sqrt{2}\lambda$, the practical limitation on the SBP due to the plotter-limited resolution is more severe than the theoretical limitation due to diffraction. For most available plotters, this is indeed the case. Possible exceptions are e-beam plotters that are capable of submicrometer resolutions, but the size of these plots is generally limited.

Logarithmic Coordinate Transformation

We illustrate our design procedure with a logarithmic transformation that has the general forms of

$$u(x) = a * \ln(x) + b,$$
$$v(y) = a * \ln(y) + b, \tag{30}$$

defined over rectangle inputs ($x_{\min} < x < x_{\max}$ and $y_{\min} < y < y_{\max}$), and where a and b are constants chosen so that $u(x_{\min}) = x_{\min}$, $u(x_{\max}) = x_{\max}$, $v(y_{\min}) = y_{\min}$, and $v(y_{\max}) = y_{\max}$. This choice of the constants a and b ensures relatively short lateral displacements and, thereby, high SBP_{ct}. Specifically, by choosing $x_{\min} = y_{\min} = 5$ mm and $x_{\max} = y_{\max} = 25$ mm, the maximal lateral displacement is only $\Delta_{\max} = 5.5$ mm, and thereby $\eta = 0.275$. The distance between the input and output planes, z, was chosen according to Eq. (24) as $z_{\mathrm{opt}} \approx 8$ mm. The theoretical limit on SBP_{ct} is then found from approximation (25) to be ~ 300 by 300 pixels.

If the paraxial approximation is used, Eq. (21) may be solved directly to obtain an analytic solution for the grating function as

$$\phi_{\mathrm{paraxial}}(x, y) = \frac{2\pi}{\lambda z}[a(x\ln x - x) + bx - 0.5x^2 + a(y\ln y - y) + by - 0.5y^2]. \tag{31}$$

Except for a quadratic phase $-(2\pi/\lambda)(x^2 + y^2)/2z$, the grating function of Eq. (31) is identical to the one obtained by Casasent and Psaltis.[6] In essence, this quadratic phase replaces the Fourier lens used in their system.

To find the optimal grating function without the paraxial approximation, we proceed by substituting Eqs. (30) into Eq. (20) yielding

$$\nabla^2\phi_h = \frac{2\pi}{\lambda r^3}\left(\left(\frac{a}{x} - 1\right)[z^2 + [v(y) - y]^2] + \left(\frac{a}{y} - 1\right)[z^2 + [u(x) - x]^2]\right). \tag{32}$$

Equation (32) was then solved numerically for an array of 100 by 100 points in the x–y plane. The results were then interpolated by quadratic spline polynomials, yielding a continuous 2-D grating function.

The optimal grating function can be compared to the paraxial one by determining the lateral errors in the output plane that are caused by the deviation of the actual grating vectors (the gradients of the optimal and paraxial grating functions) from the desired grating vector of Eq. (5). The results that were obtained by ray-tracing analysis (thus neglecting the diffraction from the input data) are presented in Fig. 4. It shows the lateral displacement errors, along the central vertical line in the output plane ($y = 15$ mm), for the optimal and the paraxial grating functions. As can be seen, the lateral errors are much smaller for the optimal grating function, thereby proving the effectiveness of our design procedure. If necessary,

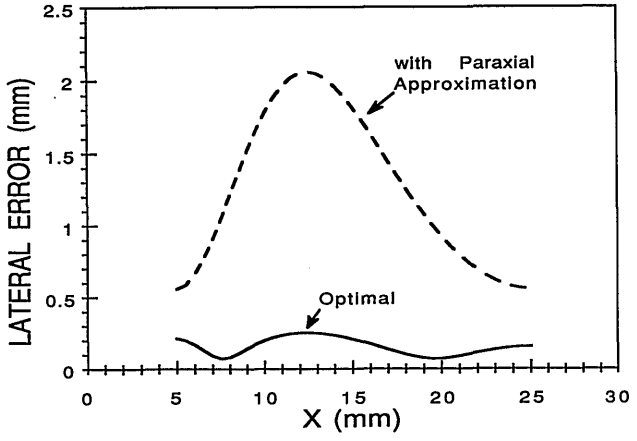

Fig. 4. Lateral errors for logarithmic coordinate transformation for a HOE with an optimal grating function (continuous curve) and for a HOE with a paraxially approximated grating function (dashed curve).

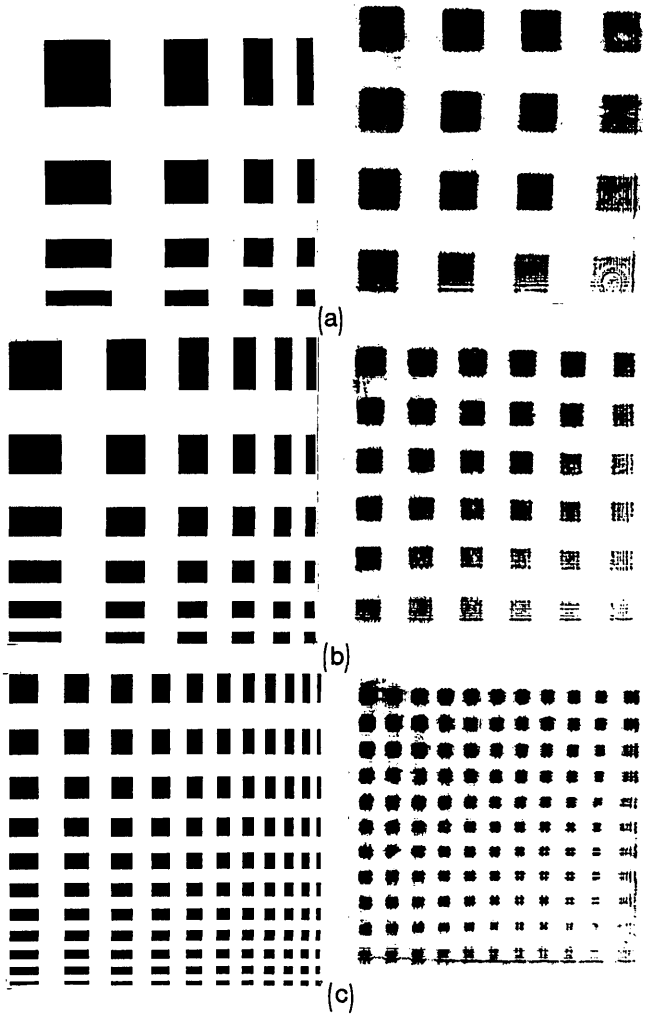

Fig. 5. Experimental results of the 2-D logarithmic geometric transformation for three different inputs. The inputs are shown on the left and the corresponding output planes are shown on the right. The actual size for all is 20 mm by 20 mm.

the lateral errors for the optimal grating function can be reduced even further by increasing the distance z. For example, if the distance z is increased to 20 mm (causing a reduction of 40% in SBP_{cr}), the lateral errors decrease by about a factor of 10. This reduction is due to the fact that the desired grating vector more nearly approximates a conserving vector for the larger distance z.

To illustrate our design procedure we recorded a COH with an optimal grating function to perform logarithmic coordinate transformations. First, a Lee-type[16] binary mask was plotted with a laser scanner, having a resolution of ~ 18 μm, directly onto photographic film. The plot was then demagnified optically by a factor of 10, yielding the desired CGH of 20 mm by 20 mm, with ~ 1.8-μm pixel size. By assuming that the minimal grating spacing contains 4 pixels, then $\Lambda_{min} \approx 7$ μm, and for $\lambda = 514.5$ nm, such a pixel size dictates, according to approximation (28), that the distance between the HOE and the output plane is $z = 150$ mm. Consequently, the maximal SBP of the transformation, governed by approximation (29), becomes only 70 by 70 pixels. The desired diffraction order of the binary CGH was imaged by a telescope composed of two high-quality Fourier lenses and interfered with a reference plane wave at an angle of 20°. This interference pattern was recorded on an Agfa 8E56 holographic plate, yielding the final off-axis HOE.

This HOE was then inserted into an optical arrangement as shown in Fig. 1, adjacent to an input transparency. The input was a scene composed of black and transparent rectangles whose width in each direction formed a geometric series. The incident illumination was $\lambda = 514.5$ nm from an argon laser, and the incident angle was 20°. The results of the logarithmic transformation are shown in Fig. 5 for three different input scenes. As expected, the outputs are composed of equal size squares, although some artifacts due to diffraction effects in the input plane are present. The reduction of intensities at the bottom right corner of the output scenes results from the conservation of energy by the transformation.

Concluding Remarks

A new method for designing HOE's that can perform general types of coordinate transformation with relatively high SBP has been presented. It is based on analytic ray tracing and a geometric shadow approximation that can be confirmed by the saddle-point approximation to the Fresnel–Kirchhoff integral. Unlike earlier designs, no paraxial approximation was necessary. The design yields an optimal solution for the grating vector of the HOE, which could then be exploited to derive an optimal grating function that may be recorded as a CGH or a COH. To illustrate the design procedure, a HOE that can perform 2-D logarithmic coordinate transformations was designed, realized, and evaluated both theoretically and experimentally. The element whose size was 20 mm by 20 mm could process input data of ~ 70 by 70 pixels in parallel at an arbitrarily high rate and hence has a high throughput. The SBP may be increased by resorting to plotters with higher resolution, such as an electron-beam recorder, or by increasing the size of the HOE.

References

1. O. Bryngdahl, "Geometrical transformation in optics," J. Opt. Soc. Am. **64,** 1092–1099 (1974).
2. G. Hausler and N. Streibl, "Optical compensation of geometrical distortion by a deformable mirror," Opt. Commun. **42,** 381–385 (1982).
3. J. Cederquist and A. M. Tai, "Computer-generated holograms for geometric transformations," Appl. Opt. **23,** 3099–3104 (1984).
4. D. Casasent, S. F. Xia, A. J. Lee, and J. Z. Song, "Real-time deformation invariant optical pattern recognition using coordinate transformations," Appl. Opt. **26,** 938–942 (1987).
5. Y. Saito, S. Komatsu, and H. Ohzu, "Scale and rotation invariant real time optical correlator using computer generated hologram," Opt. Commun. **47,** 8–11(1983).

6. D. Casasent and D. Psaltis, "Deformation invariant, space-variant optical pattern recognition," Prog. Opt. **17,** 289–356 (1978).
7. S. K Case, P. R. Haugen, and O. J. Løkberg, "Multifacet holographic optical elements for wave front transformations," Appl. Opt. **20,** 2670–2675 (1981).
8. M. A. Stuff and J. N. Cederquist, "Coordinate transformations realizable with multiple holographic optical elements," J. Opt. Soc. Am. A **7,** 977–981 (1990).
9. E. Hasman and A. A. Friesem, "Analytic optimization for holographic optical elements," J. Opt. Soc. Am. A **6,** 62–72 (1989).
10. J. W. Goodman, *Introduction to Fourier Optics* (McGraw-Hill, New York, 1968).
11. M. Born and E. Wolf, *Principles of Optics* (Pergamon, New York, 1965).
12. M. Becker, *The Principles and Applications of Variational Methods* (MIT Press, Cambridge, Mass., 1975).
13. J. W. Goodman, "Linear space-variant optical data processing," in *Optical Information Processing,* S. H. Lee, ed. (Springer-Verlag, New York, 1981).
14. R. K. Kostuk, J. W. Goodman, and L. Hesselink, "Design considerations for holographic optical interconnects," Appl. Opt. **26,** 3947–3953 (1987).
15. J. Kedmi and A. A. Friesem, "Optimized holographic optical elements," J. Opt. Soc. Am. A **3,** 2011–2018 (1986).
16. W. H. Lee, "Binary synthetic holograms," Appl. Opt. **13,** 1677–1682 (1974).